2014

The Impact of Changing Surface Ocean Conditions on the Dissolution of Aerosol Iron

Matthew P. Fishwick

Peter N. Sedwick
Old Dominion University, Psedwick@odu.edu

Maeve C. Lohan

Paul J. Worsfold

Kristen N. Buck

See next page for additional authors

Original Publication Citation

Fishwick, M.P., Sedwick, P.N., Lohan, M.C., Worsfold, P.J., Buck, K.N., Church, T.M., & Ussher, S.J. (2014). The impact of changing surface ocean conditions on the dissolution of aerosol iron. *Global Biogeochemical Cycles, 28*(11), 1235-1250. doi: 10.1002/2014GB004921

AGU PUBLICATIONS

Global Biogeochemical Cycles

RESEARCH ARTICLE
10.1002/2014GB004921

The impact of changing surface ocean conditions on the dissolution of aerosol iron

Matthew P. Fishwick[1], Peter N. Sedwick[2], Maeve C. Lohan[1], Paul J. Worsfold[1], Kristen N. Buck[3,4], Thomas M. Church[5], and Simon J. Ussher[1]

[1]School of Geography, Earth, and Environmental Sciences, University of Plymouth, Plymouth, UK, [2]Ocean, Earth, and Atmospheric Sciences, Old Dominion University, Norfolk, Virginia, USA, [3]Bermuda Institute of Ocean Sciences, St. George's, Bermuda, [4]Now at College of Marine Science, University of South Florida, St. Petersburg, Florida, USA, [5]College of Earth, Ocean, and Environment, University of Delaware, Newark, Delaware, USA

Key Points:
- Aerosol source and composition have the greatest effect on iron dissolution
- Ocean warming and acidification may not impact aerosol iron dissolution
- Strong ligands draw most of the labile aerosol iron into the soluble fraction

Correspondence to:
S. J. Ussher,
sussher@plymouth.ac.uk

Citation:
Fishwick, M. P., P. N. Sedwick, M. C. Lohan, P. J. Worsfold, K. N. Buck, T. M. Church, and S. J. Ussher (2014), The impact of changing surface ocean conditions on the dissolution of aerosol iron, *Global Biogeochem. Cycles, 28*, 1235–1250, doi:10.1002/2014GB004921.

Received 23 JUN 2014
Accepted 12 OCT 2014
Accepted article online 15 OCT 2014
Published online 15 NOV 2014

The copyright line for this article was changed on 22 JUL 2015 after original online publication.

Abstract The proportion of aerosol iron (Fe) that dissolves in seawater varies greatly and is dependent on aerosol composition and the physicochemical conditions of seawater, which may change depending on location or be altered by global environmental change. Aerosol and surface seawater samples were collected in the Sargasso Sea and used to investigate the impact of these changing conditions on aerosol Fe dissolution in seawater. Our data show that seawater temperature, pH, and oxygen concentration, within the range of current and projected future values, had no significant effect on the dissolution of aerosol Fe. However, the source and composition of aerosols had the most significant effect on the aerosol Fe solubility, with the most anthropogenically influenced samples having the highest fractional solubility (up to 3.2%). The impact of ocean warming and acidification on aerosol Fe dissolution is therefore unlikely to be as important as changes in land usage and fossil fuel combustion. Our experimental results also reveal important changes in the size distribution of soluble aerosol Fe in solution, depending on the chemical conditions of seawater. Under typical conditions, the majority (77–100%) of Fe released from aerosols into ambient seawater existed in the colloidal (0.02–0.4 μm) size fraction. However, in the presence of a sufficient concentration of strong Fe-binding organic ligands (10 n*M*) most of the aerosol-derived colloidal Fe was converted to soluble Fe (<0.02 μm). This finding highlights the potential importance of organic ligands in retaining aerosol Fe in a biologically available form in the surface ocean.

1. Introduction

During the past 20 years, extensive investigations of the marine biogeochemistry of iron (Fe) have demonstrated that this micronutrient limits primary production in vast areas of the world ocean [e.g., *Martin et al.*, 1994; *Coale et al.*, 1996; *Boyd et al.*, 2000; *Takeda and Tsuda*, 2005]. In particular, the supply of Fe controls phytoplankton growth in high-nutrient, low-chlorophyll waters, where the macronutrients nitrate and phosphate are replete. In these regions, there is the potential for increased primary production, carbon export to the deep ocean, and associated atmospheric carbon dioxide (CO_2) drawdown to be realized by increased inputs of Fe [*Martin*, 1990; *Kohfeld and Ridgwell*, 2009].

Atmospheric deposition of aerosols is an important pathway by which Fe is introduced into the surface waters of the open ocean [*Duce*, 1986; *Martin and Gordon*, 1988; *Jickells et al.*, 2005]. The percentage of the total Fe contained within aerosols that dissolves in seawater, known as the fractional solubility of aerosol Fe (%Fe_s), is known to vary substantially, depending on a number of factors. A review by *Sholkovitz et al.* [2012] notes that empirical estimates of the %Fe_s range from <0.1% to >95% (for ~1100 published values). Factors affecting the dissolution of aerosol Fe have been discussed by *Baker and Croot* [2010] and include the source and composition of the aerosols [*Bonnet and Guieu*, 2004], the particle size [*Baker and Jickells*, 2006], the concentration of particles deposited at the ocean surface [*Zhuang et al.*, 1990], and atmospheric conditioning [*Zhu et al.*, 1997]. It is therefore important to consider differences in aerosol dissolution when constructing global biogeochemical models that include Fe input to the ocean. However, most global models have thus far assumed a constant value for the %Fe_s [e.g., *Aumont et al.*, 2003; *Moore et al.*, 2004; *Parekh et al.*, 2005; *Tagliabue et al.*, 2009].

A number of studies have considered the effect of aerosol source on aerosol Fe dissolution in the marine environment and concluded that anthropogenic or combustion aerosols (e.g., unrefined fuel combustion products and biomass burning) contain Fe with a significantly higher %Fe_s compared with mineral aerosols

[e.g., *Sedwick et al.*, 2007; *Aguilar-Islas et al.*, 2010]. Therefore, the potential increase in anthropogenic aerosol emissions due to rising global population and the industrialization of developing nations [*International Energy Agency*, 2009] may be expected to increase the aeolian input of dissolved Fe (dFe) to the world ocean.

Following deposition, the physicochemical conditions of seawater, including temperature, pH, and dissolved oxygen (O_2) concentration, will impact on the dissolution of aerosol Fe and the subsequent solution speciation of aeolian Fe [*Millero et al.*, 2009]. Inorganic Fe(III) species have an extremely low solubility limit in seawater (<80 p*M*) above which they precipitate as ferric oxyhydroxides [*Liu and Millero*, 2002]. The solubility of Fe(III) species is known to increase with decreasing pH, although this trend is not strong for seawater over the pH range of 7.5–9 [*Kuma et al.*, 1996; *Liu and Millero*, 2002]. The effect of seawater temperature and dissolved O_2 concentration on Fe solubility in seawater is less clear. *Liu and Millero* [2002] report a higher solubility value for Fe(III) in 5°C seawater (0.5 n*M*) than in 25°C seawater (0.35 n*M*) and 50°C seawater (0.34 n*M*). However, *Kuma et al.* [1996] observed no change in the solubility of Fe(III) from 10°C to 20°C. In addition, the oxidation rate of the more soluble redox species Fe(II) is known to decrease with decreasing temperature, pH, and O_2 concentration [*Millero et al.*, 1987; *Croot et al.*, 2001; *Hopkinson and Barbeau*, 2007; *Breitbarth et al.*, 2010].

Iron-binding ligands in seawater play a major role in Fe biogeochemistry. By keeping Fe in solution, ligands reduce the precipitation of ferric oxyhydroxides and thus the ultimate loss of dFe from surface waters via particle scavenging and export [*Boyd and Ellwood*, 2010]. Two classes of Fe-binding ligands have been characterized: stronger ligands ("L_1"), the strongest of which occur mainly near the surface, and weaker ligands ("L_2"), which are more abundant and occur throughout the water column [*Rue and Bruland*, 1995; *Hunter and Boyd*, 2007]. These L_1 and L_2 ligands have conditional stability constants (log $K^{cond}_{FeL_i,Fe'}$, where *i* denotes the ligand class) of 11.1–13.9 and 9.7–11.95, respectively [*Gledhill and Buck*, 2012]. Numerous studies have shown that complexation by dissolved organic matter such as saccharides [*Hassler et al.*, 2011], humic substances [*Laglera and van den Berg*, 2009], and other species that make up the L_1 ligands [*Rue and Bruland*, 1995] allows Fe to exist at concentrations well in excess of the solubility of inorganic Fe(III).

Anthropogenic greenhouse gas emissions are thought to be responsible for observed increases in sea surface temperature (SST) [*Intergovernmental Panel on Climate Change*, 2013] and reductions in surface seawater pH [*Orr et al.*, 2005]. As a consequence of increased SST, the upper ocean is expected to become more stratified and less oxygenated [*Whitney et al.*, 2007; *Stramma et al.*, 2008]. Furthermore, the likely increase in anthropogenic aerosol emissions may result in an increase in the delivery of organic matter to surface waters, which may potentially contain Fe-binding ligands [*Wozniak et al.*, 2013]. These changing environmental parameters clearly have potential consequences for aerosol Fe dissolution, but the nature and magnitude of these effects are uncertain.

The experimental study described here aims to elucidate the main controls on aerosol Fe dissolution by manipulating key parameters that are likely to be affected by future environmental change, namely, SST, pH, dissolved O_2 concentration, and Fe-binding ligand concentration. Filtration using different pore size filters (0.4 μm and 0.02 μm) provided insight into the size distribution of aerosol-derived dFe in seawater leachate, as well as possible dissolution mechanisms under the range of different physicochemical conditions. In addition, experiments using bulk aerosol samples collected over a full annual cycle allowed us to assess the impact of differing aerosol sources on aerosol Fe dissolution, in relation to differing physicochemical conditions in surface seawater.

2. Methods

2.1. Seawater and Aerosol Sampling

All handling of samples and reagents was carried out under a Class 5 laminar flow hood (ISO 14644-1:1999, Bassaire or AirClean units). Ultrahigh purity (UHP, ≥18.2 MΩ cm) deionized water from Milli-Q (Millipore) or Nanopure (Barnstead) systems was used throughout this work. All plastic labware was cleaned following GEOTRACES cleaning protocols detailed by *Cutter et al.* [2010].

Seawater was collected at the Bermuda Atlantic Time-series Study (BATS) site in the Sargasso Sea (31°40′N, 64°10′W) on three cruises during the spring and summer periods (April 2010 to July 2011) on board the R/V *Atlantic Explorer*.

Polyvinylchloride 10 L Teflon-lined, external-closure Niskin-type bottles (Ocean Test Equipment) were used to collect seawater samples at the deep chlorophyll maximum (~60–120 m depth), where Fe concentrations are typically lowest [*Sedwick et al.*, 2005]. Upon recovery, samples were immediately transferred from the Niskin bottles into acid-washed 50 L low-density polyethylene (LDPE) carboys (Nalgene) inside a polyethylene-walled "clean bubble" under positive pressure. The seawater was subsequently filtered through 0.45 μm polytetrafluoroethylene (PTFE) Osmonics membrane capsules (GE Water Systems) via gravity filtration into 25 L LDPE carboys (Nalgene) and stored in the dark under ambient clean room laboratory conditions for no longer than 3 months before being used in leaching experiments. L_1-type Fe-binding ligands in all bulk seawater samples were determined by competitive ligand exchange-adsorptive cathodic stripping voltammetry prior to leaching experiments. The ligand concentrations were found to be subnanomolar (~0.8 n*M*; $n = 5$) in all samples with a log $K^{cond}_{FeL_1,Fe'}$ of ~12 (data not shown).

Four aerosol samples were collected from the Tudor Hill atmospheric observatory on the southwest coast of Bermuda (32°15.95'N, 64°52.65'W) from 13 July to 20 August 2009 (AER 1, 38 days sampling), 27 September to 11 October 2010 (AER 2, 14 days sampling), 22 February to 10 May 2010 (AER 3, 54 days sampling), and 11 October to 13 December 2010 (AER 4, 63 days sampling). To help structure the discussion, sample numbers AER 1–AER 4 were ordered to reflect the influence of North American air masses during sampling (from smallest to largest). Samples were taken from a high-volume aerosol sampler, which drew air through 8 × 10" sheets of 2.2 μm pore size quartz microfiber Whatman QMA filters (GE Healthcare). The total volume of air sampled for AER 1, AER 2, AER 3, and AER 4 over these sampling periods was 8620 m^3, 10,519 m^3, 35,356 m^3, and 24,243 m^3, respectively. The aerosol filters were previously acid washed following a method described by *Morton et al.* [2013]. The aerosol sampler was located approximately 50 m above sea level on top of a 23 m high aluminum scaffolding tower. To avoid local aerosol sources and ensure that only marine air was sampled, pumps were switched off when the wind direction was not in the onshore sector (210–315°), or if the wind speed was less than 1 m s^{-1}. A procedural field blank was taken by loading an aerosol filter into the aerosol sampler, leaving it in the sampler (with pumps off) for 5 min and then removing it. Aerosol samples were removed and placed in zip-lock bags and stored frozen at −20°C for 6–24 months before use.

2.2. Seawater Preconditioning

Separate 1 L aliquots of the 0.45 μm filtered BATS seawater were preconditioned before use in the leaching experiments. Filtered seawater aliquots used in the variable temperature experiments were equilibrated to 4°C and 25°C, using a fridge and temperature-controlled laboratory, respectively. Filtered seawater aliquots used in the variable seawater pH experiments were preconditioned by sparging with filtered air/CO_2 mixtures using mass flow controllers until a stable pH was reached (between 48 and 72 h) [*de Putron et al.*, 2011]. The sparging gas mixtures simulated equilibrium with atmospheric CO_2 concentrations of 400 ppm CO_2 (present-day conditions) and 1250 ppm CO_2 (possible future conditions), resulting in seawater pH values of 8.0 ("ambient seawater") and 7.6 ("acidified seawater"), respectively. "Total-scale" pH was calculated using the measured values of total dissolved inorganic carbon and alkalinity using "CO_2sys." Similarly, anoxic conditions (<0.1% O_2) were created by purging dissolved O_2 from filtered seawater by sparging with filtered nitrogen (N_2) gas (for leaches 3 and 4 only). Filtered seawater aliquots used in organic ligand amendment experiments were preconditioned through the addition of a strong siderophore L_1-type ligand (either 10 n*M* of aerobactin (EMC Microcollections) or desferrioxamine B (Sigma–Aldrich)) or weaker L_2-type ligands (either 10 n*M* of protoporphyrin IX (Sigma–Aldrich) or 1 μM of glucuronic acid (Sigma–Aldrich)). These ligands were intended to simulate the range of Fe-binding ligands that exist in open ocean waters and were added in concentrations in excess (~1 order of magnitude) of typical open ocean surface water concentrations in the western North Atlantic [*Cullen et al.*, 2006; *Buck et al.*, 2014] in order to observe a clear response in aerosol Fe complexation.

2.3. Aerosol Leaching Experiments

Aerosol leaching experiments were designed to replicate the process of dry deposition in the open ocean as closely as possible within the laboratory. Leaches were performed using an acid-washed filtration tower (Savillex) comprising a 47 mm diameter perfluoroalkoxy filter assembly clamp, 250 mL evacuated Teflon collection vessel, and 0.25" diameter PTFE tubing. The PTFE tubing connected the collection vessel to a vacuum pump (GAST) via a 0.2 μm Acrovent air filter (Pall Corporation) and water trap. Acid-washed 0.4 μm

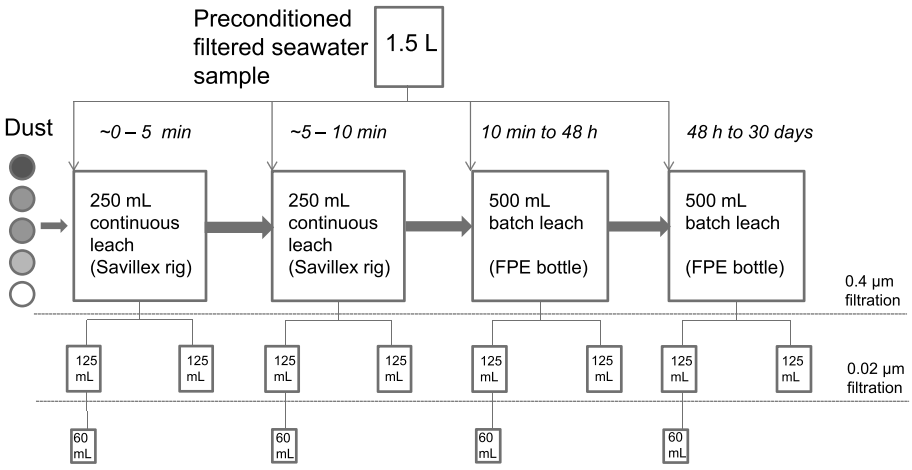

Figure 1. Summary of aerosol leaching method. Leaches 1 and 2 were continuous leaches carried out using a Savillex filtration tower, and leaches 3 and 4 were batch leaches carried out in 500 mL fluorinated polyethylene (FPE) bottles. All seawater leachate samples were filtered through 0.4 µm and 0.02 µm pore size filters to define the size distribution of dissolved iron species in solution.

pore size, 47 mm polycarbonate track-etched membrane filters (Nuclepore, GE Healthcare) were used to separate "dissolved Fe" in the aerosol leachate solutions. Triplicate subsamples from each aerosol filter sample were taken using a 20 mm diameter polished steel arch punch (Osborne) and allowed to thaw at room temperature before being used for each different treatment in the aerosol leaching experiments.

The leaching process (Figure 1) involved four sequential leaches to test different equilibration times (leach 1 = 0–5 min, leach 2 = 5–10 min, leach 3 = 10 min–48 h, and leach 4 = 48 h–30 days). These leaching times were chosen to represent the typical range of residence times for aerosol particles in the upper surface ocean. For leach 1, a 20 mm diameter aerosol filter subsample was placed on a polycarbonate filter mounted within the filtration tower (under vacuum). Then 250 mL of preconditioned filtered seawater was poured over the aerosol filter in a continuous leaching process, lasting 5 min, with the resulting leachate collected. This process was repeated for leach 2 using the same aerosol subsample used in leach 1. Leaches 3 and 4 were batch leaches where the same aerosol subsample and polycarbonate filters used in leaches 1 and 2 were placed in fluorinated polyethylene (FPE, Nalgene) bottles with 500 mL of preconditioned filtered seawater for 48 h and 30 days for leaches 3 and 4, respectively (Figure 1). Previous studies employing an aerosol batch leach methodology have observed only negligible adsorption of dFe to bottle walls when fluorinated polymer bottles were used [*Séguret et al.*, 2011]. To further minimize the effect of wall adsorption of dFe, the FPE bottles were first preconditioned for 24–72 h with filtered BATS seawater before batch leaches took place. To minimize the influence of ultraviolet light on Fe dissolution, leaches 1 and 2 were carried out under artificial light only, whereas leaches 3 and 4 were stored in darkness. The seawater leachate solutions that passed through the 0.4 µm filter membrane in each sequential leach were subsequently decanted into acid-washed 125 mL LDPE bottles (Nalgene). The entire leaching process was conducted in triplicate for every experimental treatment.

To determine "colloidal Fe" (cFe) and "soluble Fe" (sFe), 125 mL of seawater leachate samples were filtered through 0.02 µm pore size, 25 mm diameter aluminum oxide Whatman Anotop syringe filters (GE Healthcare) and collected in acid-washed 60 mL LDPE bottles (Nalgene) (Figure 1). In this study, following the definitions of *Wu et al.* [2001], dFe is defined as the $<$0.4 µm fraction, and sFe is defined as the $<$0.02 µm fraction. Colloidal Fe is thus inferred from the difference between dFe and sFe, representing the 0.02–0.4 µm size fraction (i.e., cFe = dFe-sFe). The Anotop filters used for ultrafiltration of aerosol leachate were set up and conditioned following the in-line filtration method detailed by *Ussher et al.* [2010]. Following aerosol leaches, all seawater leachate samples (including blanks) were acidified to pH ~1.7 using HCl (Romil, UpA) and stored for $>$1 year before analysis. In addition to leachate samples, process blanks were prepared by passing ambient filtered seawater over a procedural field blank subsample (section 2.1) and a 47 mm polycarbonate filter. Following analysis, the Fe concentrations of the relevant process blanks were subtracted from Fe concentrations of all leachate samples. The dFe concentrations of the process blanks were typically $<$0.1 n*M*.

2.4. Determination of Iron in Seawater Leachates Using Flow Injection With Chemiluminescence

The concentrations of dFe and sFe in seawater leachate solutions were determined using flow injection with chemiluminescence detection (FI-CL) inside a Class 100 clean room (ISO 9001:2008), based on the method described by *Obata et al.* [1993]. Briefly, seawater leachate samples were buffered in-line to pH 3.5 with 0.35 *M* ammonium acetate (Romil, SpA) then loaded on a chelating column containing Toyopearl AF-Chelate-650 M iminodiacetate resin (IDA, Tosoh Bioscience). The seawater matrix major cations were removed using a 0.012 *M* HCl (Romil, SpA) rinse and then Fe was eluted from the column using 0.23 *M* HCl (Romil, SpA). The acid/analyte eluent was then mixed with 0.25 m*M* luminol, 0.5 *M* ammonium hydroxide, and 0.3 *M* hydrogen peroxide to initiate the oxidation of luminol [*Rose and Waite*, 2001], which produced a chemiluminescence signal detected by a photomultiplier tube (Hamamatsu).

Iron concentrations were quantified using the method of standard additions to low-Fe seawater ($<$0.35 n*M* dFe), subsampled from the original filtered seawater used for leaches (four sets of concentration ranges were used: 0.6–12 n*M*, 0.6–5 n*M*, 0.6–2.4 n*M*, and 0.2–1.4 n*M*; $n = 6$). All standards and samples were analyzed in triplicate. The accuracy of the method was checked daily by analyzing SAFe and GEOTRACES reference seawater and comparing the determined concentrations with consensus values: SAFe S = 0.091 ± 0.008 n*M* ($n = 29$), SAFe D2 = 0.910 ± 0.022 n*M* ($n = 29$), and GEOTRACES GD = 0.98 ± 0.10 n*M* ($n = 22$), (K. Bruland, unpublished data, 2008, available from the Bruland Research Laboratory at http://es.ucsc.edu/~kbruland/GeotracesSaFe/kwbGeotracesSaFe.html). The concentrations of Fe in reference seawater determined using this FI-CL system were typically within the range of the consensus values (SAFe S = 0.10 n*M* ($n = 3$), SAFe D2 = 0.85–0.91 n*M* ($n = 4$), and GEOTRACES GD = 0.83–0.99 n*M* ($n = 8$)). Analytical precision was typically better than ±5% relative standard deviation (RSD) for all standards, reference seawater, and samples.

2.5. Total Trace Metal Determination by Inductively Coupled Plasma Mass Spectrometry

Triplicate subsamples of AER 1–AER 4 and blanks were completely digested using concentrated hydrofluoric acid (28.9 *M* HF, Seastar, Baseline), concentrated nitric acid (15.8 *M* HNO_3, Seastar, Baseline), and heat [*Morton et al.*, 2013] at the University of Delaware. As acid digestion is a destructive process, it was necessary to use different subsamples of each aerosol sample in the aerosol leaching experiments and use the mean total Fe amount in fractional solubility calculations. Total element determinations were subsequently performed on the digests at Old Dominion University using an Element 2 (Thermo Fisher) inductively coupled plasma–mass spectrometer (ICP-MS) in medium resolution mode. Samples were spiked with indium (^{115}In) as an internal standard. Calibration standards were made up using a multielemental standard (QC Standard 4, PlasmaCal containing aluminum (Al), titanium (Ti), manganese (Mn), vanadium (V), chromium (Cr), Fe, cobalt (Co), nickel (Ni), copper (Cu), zinc (Zn), cadmium (Cd), antimony (Sb), and lead (Pb)) in the same 2% (vol/vol) HNO_3 matrix as the aerosol digest solutions.

2.6. Air Mass Back Trajectory Analysis

Air mass back trajectories were simulated using the Hybrid Single-Particle Lagrangian Integrated Trajectory (HYSPLIT) model developed by the U.S. National Oceanic and Atmospheric Administration (available for download at http://ready.arl.noaa.gov/hyreg/HYSPLIT_pchysplit.php). Ten-day back trajectories at altitudes of 50 m, 500 m, and 2000 m were performed for each day within the period over which aerosol samples were collected. Daily back trajectories were used in the cluster analysis function of HYSPLIT to generate 10 mean back trajectories for each aerosol sampling period.

3. Results and Discussion

3.1. Aerosol Sample Characterization

The aerosol samples collected at Tudor Hill represent a seasonal-scale time series comprising a summer sample (AER 1), an autumn sample (AER 2), a spring sample (AER 3), and a winter sample (AER 4). Daily 500 m elevation 10 day air mass back trajectories for each day of the collection period of each aerosol sample are provided in Figure 2. Air mass back trajectories modeled at 50 m and 2000 m elevations (not shown) were similar to those modeled at 500 m. The back trajectories for AER 1 (Figure 2a), collected between July and August 2009 and AER 2 (Figure 2b), collected between September and October 2010, suggest that the air had predominately traveled from the east, entraining soil dust from North Africa, as is typical for aerosols in the Bermuda region during summer [*Sedwick et al.*, 2007]. The back trajectories for AER 3 (Figure 2c), collected

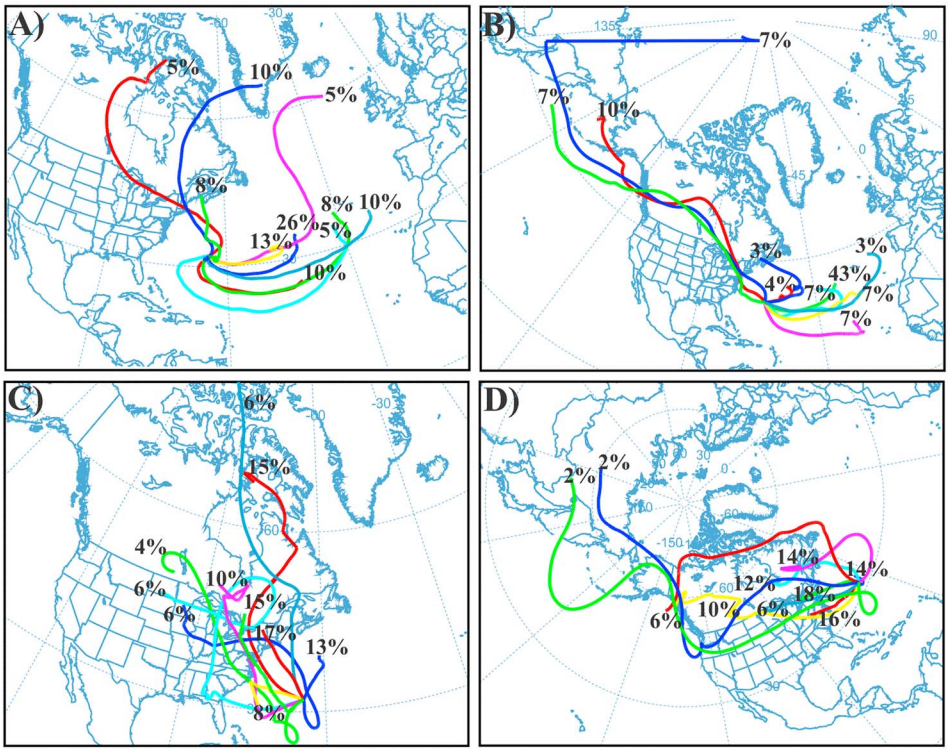

Figure 2. Mean air mass back trajectory clusters generated from daily 500 m 10 day back trajectories from Tudor Hill using the Hybrid Single-Particle Lagrangian Integrated Trajectory (HYSPLIT) model for the following sampling periods: (a) 13 July to 20 August 2009 (AER 1), (b) 27 September to 11 October 2010 (AER 2), (c) 22 February to 10 May 2010 (AER 3), and (d) 11 October to 13 December 2010 (AER 4). Ten mean back trajectory clusters are shown for each sample with the proportion of total trajectories used in each cluster shown beside each mean back trajectory cluster (totals may not equal 100% due to rounding).

from February to May 2010 and AER 4 (Figure 2d), collected between October and December 2010, suggest that the air had predominately traveled from the northwest, entraining aerosols from North America. These results are consistent with time series aerosol observations from Bermuda over a number of decades [*Duce and Hoffman*, 1976; *Chen and Duce*, 1983; *Anderson et al.*, 1996; *Sholkovitz et al.*, 2009].

To gain an appreciation of the relative contributions of anthropogenic versus crustal materials to the aerosols, total masses of Fe, V, Ni, Cu, Pb, and Sb in the aerosol samples (Table 1) were normalized to the mass of Al, and the resulting ratios were compared with those of average continental crust [*Taylor and McLennan*, 1995] to calculate enrichment factors (Table 2). Samples collected in the winter (i.e., AER 4) were more enriched (enrichment factors >10) in V, Ni, Cu, Pb, and Sb relative to aerosols collected in the summer (i.e., AER 1 and AER 2). These results are consistent with the back trajectory models (Figure 2) and agree with the suggestion of *Sedwick et al.* [2007] that marine air over the Sargasso Sea contains a greater proportion of anthropogenic combustion products (relative to continental soil dust) in the winter. Summer Fe and Al atmospheric loadings were higher than those determined in the winter (Table 1), consistent with previous work that has shown high-Fe and -Al loadings in air masses dominated by lithogenic aerosols, relative to anthropogenic materials [*Baker et al.*, 2006; *Buck et al.*, 2010a; *Séguret et al.*, 2011].

3.2. Effect of Seawater Temperature, pH, and Deoxygenation on Aerosol Iron Dissolution

The total dFe leached from aerosols into preconditioned seawater samples of different temperature, pH, and O_2 concentration was calculated from the process-blank-corrected dFe concentrations and volumes of seawater leachate (Figure 3). An alternative representation of these results, as fractional solubilities of aerosol Fe (total dFe released into solution divided by total aerosol Fe), is shown in Figure 4.

The mean total dFe leached from each aerosol sample (AER 1–AER 4) into 4°C and 25°C seawater is shown in Figure 3a. The mean total dFe is the sum of all dFe released into seawater during the four sequential leaches and ranged from 0.7 ± 0.2 nmol to 4 ± 2 nmol for AER 1–AER 4 under these different seawater

Table 1. Total Trace Metal Masses[a] Contained in Aerosol Subsamples and Atmospheric Loading of Trace Metals in Sampled Air[b]

Aerosol Sample	Sample Period	Total Mass of Trace Metal in Aerosol Subsample (ng)							Concentration of Trace Metal in Sampled Air (pmol m^{-3})						
		Al	Fe	V	Ni	Cu	Pb	Sb	Al	Fe	V	Ni	Cu	Pb	Sb
AER 1	13 Jul to 20 Aug 2009	16,200 ±700	9,180 ±300	41.0 ±0.4	17.0 ±0.6	14.8 ±0.4	18.0 ±0.6	2.65 ±0.2	8,800 ±400	2,400 ±70	12 ±0.1	4.3 ±0.2	3.4 ±0.1	1.3 ±0.04	0.32 ±0.02
AER 2	27 Sep to 11 Oct 2010	21,000 ±500	12,300 ±100	82.0 ±5	32.0 ±1	31.1 ±3	28.8 ±0.5	5.21 ±0.01	9,400 ±200	2,700 ±30	19 ±1	6.6 ±0.2	5.9 ±0.5	1.7 ±0.03	0.52 ±0.001
AER 3	22 Feb to 10 May 2010	30,000 ±900	18,600 ±200	169 ±40	76.0 ±10	92.9 ±30	146 ±30	24.6 ±1	4,000 ±100	1,200 ±10	12 ±3	5 ±1	5 ±1	2.5 ±1	0.73 ±0.04
AER 4	11 Oct to 13 Dec 2010	8,840 ±900	4,870 ±100	73.0 ±4	31.0 ±1	47.5 ±3	75.0 ±9	14.4 ±0.3	1,700 ±200	460 ±10	7.5 ±0.4	2.8 ±0.1	3.9 ±0.2	1.9 ±0.2	0.62 ±0.01

[a]Total mean masses (ng) of aluminum (Al), iron (Fe), vanadium (V), nickel (Ni), copper (Cu), lead (Pb), and antimony (Sb) in triplicate subsamples of each aerosol sample. Standard deviations from mean masses (±1σ) represent masses of metals determined for three subsamples of the same aerosol sample.
[b]Mean concentrations (pmol m^{-3}) of Al, Fe, V, Ni, Cu, Pb, and Sb in sampled air calculated using the total mean masses of trace metals in each aerosol subsample and the total volume of air passed through each sample filter over the sampling period. Standard deviations from mean concentrations (±1σ) represent the uncertainty of trace metal mean mass measurements only.

conditions. The uncertainty in the mean total dFe values of a given sample was dominated by differences between replicate leaches of subsamples of the same aerosol sample, with an RSD of 13–45%, rather than replicate Fe analyses of the same leachate solution, with an RSD of 5–6%, which is in accord with results of other studies [e.g., *Morton et al.*, 2013]. Most of the aerosol Fe was released into solution during the first leach, with progressively less Fe released in the subsequent sequential leaches. It is clear that the dissolution of Fe from aerosols occurred rapidly; the majority (84–94%) of the aerosol-derived dFe was released within the first 10 min of contact with seawater. Similar kinetics were observed for all leaches assessed in this study and in other studies of aerosol Fe solubility [e.g., *Buck et al.*, 2006; *Wu et al.*, 2007]. Importantly, the differences in the mean total dFe released into 4°C versus 25°C seawater were not statistically significant (two-tailed t test, $p > 0.05$) for any of the aerosol samples, suggesting that seawater temperature does not exert a major control on the dissolution of aerosol Fe.

The mean total sFe (<0.02 μm) leached from each aerosol sample (AER 1–AER 4) into 4°C and 25°C seawater is shown in Table 3. The mean total sFe from the four sequential leaches into these different seawater conditions ranged from 0.04 nmol to 0.41 nmol for AER 1–AER 4. The colloidal Fe size fraction (cFe, 0.02–0.4 μm) can be inferred by comparing the dFe and sFe in the seawater leachate. For all leaches, the majority (77–97%) of dFe released from the aerosols into the seawater leachate resided in the cFe size fraction (Table 3). It should be noted that these data represent the size distribution of dFe in solution following leaching from aerosols, not the amount of sFe and cFe that has been directly leached from the aerosols. The mean total sFe in solution leached from the aerosols at 4°C was greater than that leached at 25°C for aerosols AER 2 and AER 3. Conversely, for AER 1 and AER 4, the mean total sFe leached from the aerosols at 25°C seawater was greater than that leached at 4°C. However, the differences in the mean total sFe in the leachate using 4°C seawater versus 25°C seawater were not statistically significant (two-tailed t test, $p > 0.05$) when the differences in dFe for replicate leaches are taken into account, suggesting that seawater temperature does not exert a major control on the size distribution (sFe versus cFe) of dFe in the aerosol leachate solutions.

The mean total quantities of dFe leached from each aerosol sample (AER 1–AER 4) into ambient seawater (25°C, pH 8.0, oxygenated), acidified seawater (pH 7.6, sparged with air/CO_2 mixture, 1250 ppm CO_2), and "anoxic seawater" (sparged with N_2 for leaches 3 and 4) are shown in Figure 3b. The mean total dFe is the sum of all dFe released during the four leaches and ranged from 0.6 ± 0.2 nmol to 5 ± 2 nmol for AER 1–AER 4, for these different seawater conditions. Our results show that the total dFe released into acidified and

Table 2. Trace Metal to Aluminum Mass Ratios[a] and Trace Metal Enrichment Factors Relative to Upper Continental Crust Abundances[b]

Aerosol Sample	Mass Ratio						Enrichment Factors					
	Fe/Al	V/Al	Ni/Al	Cu/Al	Pb/Al	Sb/Al	Fe	V	Ni	Cu	Pb	Sb
AER 1	0.568	0.00254	0.00105	0.000917	0.00111	0.000164	1.3	3.4	4.2	2.9	4.5	66
	±0.06	±0.00004	±0.00006	±0.00004	±0.00006	±0.00002	±0.1	±0.05	±0.2	±0.1	±0.2	±7
AER 2	0.584	0.00391	0.00152	0.00148	0.00137	0.000248	1.3	5.2	6.1	4.8	5.5	100
	±0.01	±0.0003	±0.00008	±0.0002	±0.00003	±0.000001	±0.02	±0.5	±0.3	±0.6	±0.1	±0.4
AER 3	0.620	0.00563	0.00253	0.00310	0.00486	0.000820	1.4	7.5	10	10	20	330
	±0.008	±0.002	±0.0005	±0.001	±0.002	±0.00007	±0.02	±2	±2	±4	±6	±30
AER 4	0.551	0.00826	0.00351	0.00537	0.00848	0.00163	1.3	11.0	14	17	34	660
	±0.02	±0.0007	±0.0003	±0.0005	±0.002	±0.00005	±0.05	±1	±1	±1	±6	±20

[a]Iron/aluminum (Fe/Al), vanadium/aluminum (V/Al), nickel/aluminum (Ni/Al), copper/aluminum (Cu/Al), lead/aluminum (Pb/Al), and antimony/aluminum (Sb/Al) mass ratios calculated by dividing the total mean mass of each trace metal with the total mean mass of aluminum in each aerosol subsample. Standard deviations from mean mass ratios (±1σ) represent the uncertainty of trace metal mean mass measurements only.

[b]Iron (Fe), vanadium (V), nickel (Ni), copper (Cu), lead (Pb), and antimony (Sb) enrichment factors were calculated by dividing trace metal/aluminum mass ratios of aerosol samples by trace metal/aluminum ratios found in the upper continental crust. Abundances of trace metals in the upper continental crust taken from *Taylor and McLennan* [1995] and used to calculate mass ratios (Fe/Al = 0.4, V/Al = 0.0007, Ni/Al = 0.0002, Cu/Al = 0.0003, Pb/Al = 0.0002, and Sb/Al = 0.000002). Standard deviations from mean enrichment factors (±1σ) represent the uncertainty of trace metal mean mass measurements only.

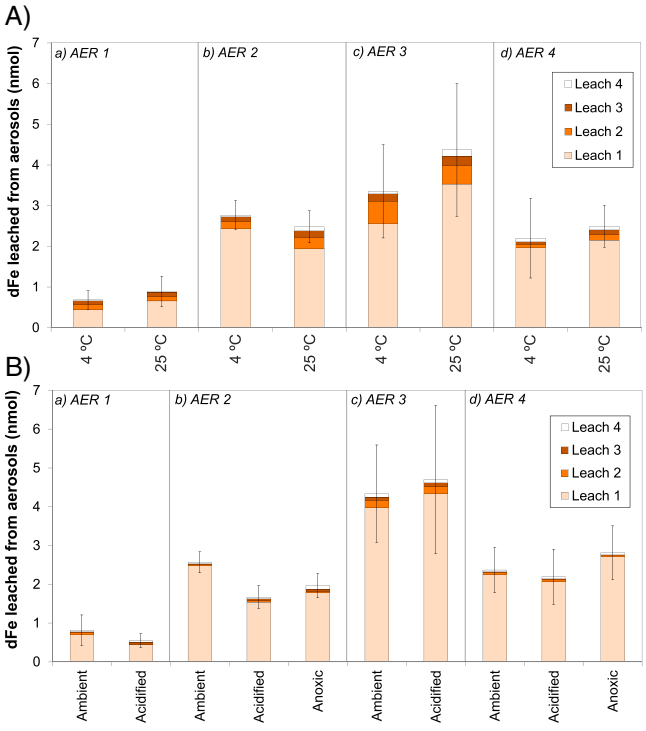

Figure 3. The mean total dissolved iron (dFe, nmol) leached from aerosol samples AER 1, AER 2, AER 3, and AER 4 during three replicate leaches with (a) 4°C and 25°C seawater and (b) ambient seawater (25°C, pH 8.0, oxygenated), acidified seawater (25°C, pH 7.6, sparged with air enriched in carbon dioxide), and anoxic seawater (25°C, sparged with nitrogen gas for leaches 3 and 4). The error bars represent the standard deviation (±1σ) on the mean total dFe leached from replicate subsamples of the same aerosol sample. Segments of each bar show the amount of dFe leached during each sequential aerosol leach (i.e., leaches 1–4). Sequential leaches 1, 2, 3, and 4 represent the following time periods for seawater that was exposed to aerosols: 0–5 min, 5–10 min, 10 min–48 h, and 48 h–30 days, respectively.

anoxic seawater was not statistically different (two-tailed *t* test, $p > 0.05$) from the total dFe released into ambient seawater for all aerosol samples.

The mean total sFe in the seawater leached from each aerosol sample (AER 1–AER 4) into ambient, acidified, and anoxic seawater is shown in Table 3. The mean total sFe from the four sequential leaches into these different seawater conditions ranged from 0.02 nmol to 0.16 nmol for AER 1–AER 4. In all cases, the majority (92–98%) of dFe in the seawater leachate solutions resided in the cFe size fraction (Table 3). There were some differences observed between samples: for example, the mean total sFe leached into ambient seawater was greater than that leached into acidified seawater for two of the four aerosol samples (AER 2 and AER 3), whereas the opposite was observed for AER 1 and AER 4. However, similar to the dFe results, the differences in the mean total sFe in the various seawater leachate samples were not statistically significant (two-tailed *t* test, $p > 0.05$) when the differences in dFe for replicate leaching experiments are taken into account.

Thus, our experimental results suggest that seawater temperature,

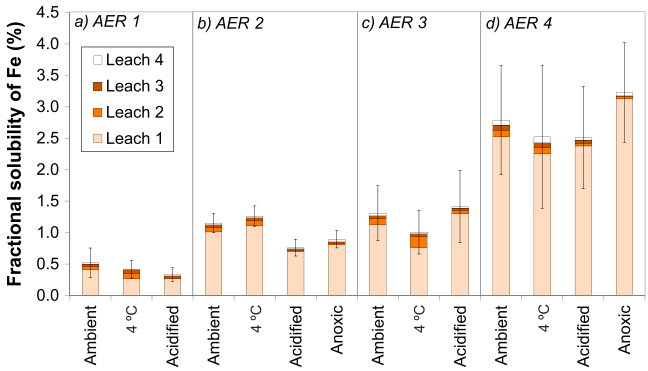

Figure 4. Fractional solubility (%) of iron (Fe) from aerosol samples AER 1, AER 2, AER 3, and AER 4 leached with ambient seawater (combined mean of the temperature experiment and pH and deoxygenation experiment, 25°C, pH 8.0, oxygenated), 4°C seawater, acidified seawater (25°C, pH 7.6, sparged with air enriched in carbon dioxide), and anoxic seawater (25°C, sparged with nitrogen gas for leaches 3 and 4). The error bars represent the standard deviation (±1σ) on the mean fractional solubility of Fe leached from replicate subsamples of the same aerosol sample. Segments of each bar show the fractional solubility of each sequential aerosol leach (i.e., leaches 1–4). Sequential leaches 1, 2, 3, and 4 represent the following time periods for seawater that was exposed to aerosols: 0–5 min, 5–10 min, 10 min–48 h, and 48 h–30 days, respectively.

pH (as controlled by pCO_2), and O_2 concentration did not exert a major control on the dissolution of aerosol Fe, nor on the size distribution of aerosol-derived dFe in seawater, within the experimental uncertainties and ranges of the parameters examined. These observations are in accord with those of *Kuma et al.* [1996], who reported no difference in the solubility of inorganic Fe(III) in seawater at 10°C versus 20°C. In contrast, however, *Liu and Millero* [2002] reported higher solubility of Fe(III) seawater at 5°C versus 25°C (0.5 ± 0.07 n*M* for 5°C seawater and 0.35 ± 0.06 n*M* for 25°C seawater). Other studies have demonstrated an increase in the solubility of inorganic Fe with decreasing pH [*Byrne and Kester*, 1976; *Kuma et al.*, 1996; *Liu and Millero*, 2002]. However, consistent with this study, *Liu and Millero* [2002] report that Fe solubility does not change in the pH range of 7.5–9, due to the dominance of the neutrally charged species $Fe(OH)_3°$ [*Liu and Millero*, 1999]. It should be noted that in the cases of *Liu and Millero* [2002] and *Byrne and Kester* [1976], equilibrium conditions were represented, whereas our leach experiments are not likely to represent equilibrium conditions. Data from our study also agree with empirical data that suggest little difference in the dissolution of aerosol Fe in seawater (pH ~8) versus UHP (≥18.2 MΩ cm, pH 5.6) deionized water [*Aguilar-Islas et al.*, 2010; *Buck et al.*, 2013].

Table 3. The Mean Total (nmol) of Dissolved Iron (dFe), Colloidal Iron (cFe), and Soluble Iron (sFe) Leached From Aerosol Samples AER 1, AER 2, AER 3, and AER 4 During Three Replicate Leaches With Seawater[a]

Aerosol Sample	Seawater Condition	Total Fe Leached From Aerosols (nmol)			Colloidal Proportion of dFe (%)
		dFe	cFe	sFe	
AER 1	25°C	0.9 ± 0.4	0.68	0.20	77%
AER 1	4°C	0.7 ± 0.2	0.64	0.037	94%
AER 1	Ambient (25°C, pH 8.0, oxygenated)	0.8 ± 0.4	0.80	0.016	98%
AER 1	Acidified (pH 7.6)	0.6 ± 0.2	0.51	0.043	92%
AER 2	25°C	2.4 ± 0.4	2.3	0.15	94%
AER 2	4°C	2.8 ± 0.4	2.3	0.41	85%
AER 2	Ambient (25°C, pH 8.0, oxygenated)	2.6 ± 0.3	2.5	0.09	97%
AER 2	Acidified (pH 7.6)	1.7 ± 0.3	1.6	0.052	97%
AER 2	Anoxic	2.0 ± 0.3	1.9	0.060	97%
AER 3	25°C	4.3 ± 1.6	4.2	0.12	97%
AER 3	4°C	3.3 ± 1.1	3.1	0.22	93%
AER 3	Ambient (25°C, pH 8.0, oxygenated)	4.3 ± 1.3	4.2	0.16	96%
AER 3	Acidified (pH 7.6)	4.7 ± 1.9	4.6	0.11	98%
AER 4	25°C	2.5 ± 0.5	2.2	0.23	91%
AER 4	4°C	2.2 ± 1.0	2.0	0.15	93%
AER 4	Ambient (25°C, pH 8.0, oxygenated)	2.4 ± 0.6	2.3	0.055	98%
AER 4	Acidified (pH 7.6)	2.2 ± 0.7	2.1	0.055	97%
AER 4	Anoxic	2.8 ± 0.7	2.8	0.043	98%

[a]The 25°C seawater, 4°C seawater, ambient seawater from the pH and deoxygenation experiment (25°C, pH 8.0, oxygenated), acidified seawater (25°C, pH 7.6, sparged with air enriched in carbon dioxide), and anoxic seawater (25°C, sparged with nitrogen gas for leaches 3 and 4). Standard deviations (±1σ) from the mean total Fe leached from replicate subsamples of the same aerosol sample are shown for dFe.

Given the year 2100 projections for average SST to increase by 1°C [*Meehl et al.*, 2007], seawater pH to decrease by 0.25 [*Caldeira and Wickett*, 2003], and oceanic oxygen minimum zones to expand [*Shaffer et al.*, 2009], our data suggest that such changes will not significantly impact on aerosol Fe dissolution in surface ocean waters. However, it should be stressed that the combined effect of these changes, or the impact of such changes on other factors that impact aerosol Fe dissolution, cannot be ruled out. Our findings have important implications for modeling the impact of future changes in aerosol input to the global cycling of Fe and carbon, as well as phytoplankton growth and community structure. Specifically, our experimental results suggest that to a first approximation, models do not need to consider that aerosol Fe dissolution will vary as a function of projected variations in seawater temperature, pH, or oxygen saturation. While seawater temperature, pH, and O_2 concentration had no significant effect on aerosol Fe dissolution, we observed pronounced differences in aerosol Fe solubilities for aerosols from different source regions with different bulk compositions.

3.3. Effect of Aerosol Source and Composition on Aerosol Iron Dissolution

Seawater leaching of aerosol samples of different source and composition resulted in different fractional solubilities of aerosol Fe under all conditions (Figure 4). Indeed, there is nearly an order of magnitude difference in the $\%Fe_s$ for the more "anthropogenic"-type aerosol (AER 4) relative to the "mineral dust"-type aerosol (AER 1). The operationally defined $\%Fe_s$ for aerosol AER 1 was consistently lower ($0.3 \pm 0.1\%$ to $0.5 \pm 0.2\%$) than that for aerosol AER 4 ($2.5 \pm 0.8\%$ to $3.2 \pm 0.8\%$) under all physicochemical conditions of the seawater leaching experiments. The dependence of aerosol Fe solubility on aerosol type and source has been noted in previous studies [*Sedwick et al.*, 2007; *Sholkovitz et al.*, 2009; *Buck et al.*, 2010b; *Séguret et al.*, 2011; *Shelley et al.*, 2012; *Baker et al.*, 2013; *Wozniak et al.*, 2013]. It has been suggested that the elevated $\%Fe_s$ in anthropogenically influenced aerosols reflects acidic processing at the particle surface [*Meskhidze et al.*, 2005; *Hsu et al.*, 2010], the presence of labile Fe sulfates and other soluble Fe phases [*Oakes et al.*, 2012], and the tendency for anthropogenic aerosols to be smaller than mineral dust particles [*Chen and Siefert*, 2004; *Jang et al.*, 2007]. Conversely, mineral aerosol particles tend to be larger, with much of the Fe contained in refractory minerals [*Desboeufs et al.*, 2005].

Sholkovitz et al. [2009] show a linear relationship between the $\%Fe_s$ and the V/Al mass ratios of bulk aerosol samples collected over the Sargasso Sea. That linear relationship and the V/Al mass ratios of bulk aerosol samples collected in this study were used to predict fractional solubilities in ambient seawater; these predictions were then compared with empirically determined fractional solubilities. While absolute values of the predicted and determined fractional solubilities differed (predicted values of 1.4%, 2.0%, 2.7%, and 3.8% for AER 1, AER 2, AER 3, and AER 4, respectively, versus observed values of 0.5%, 1.2%, 1.3%, and 2.8% for AER 1, AER 2, AER 3, and AER 4, respectively), the predicted trend of increasing solubility with increasing V/Al mass ratios matched the empirical values. Thus, our results indicate greater $\%Fe_s$ in aerosols containing a larger proportion of anthropogenic material.

While this study is unable to provide insight into the mechanism of enhanced Fe solubility in non-soil-dust aerosols, the results add to the existing evidence that Fe in anthropogenic aerosols is more soluble than Fe in soil-derived mineral dust and that this variability dominates over potential changes in the fundamental parameters of temperature, pH, and O_2 concentration of the seawater in which aerosols are deposited. These results suggest that the potential for an increase in anthropogenic aerosol emissions accompanying the rising global population and the industrialization of developing nations [*International Energy Agency*, 2009] could conceivably increase the atmospheric flux of dFe to the ocean and may exert significant regional-scale impacts [*Sholkovitz et al.*, 2009]. However, when considering a total flux including refractory material, soil dust is likely to continue to dominate the total global aerosol Fe deposition [*Prospero et al.*, 2002], and therefore, the global importance of anthropogenic aerosol Fe input is likely to remain marginal. These results reinforce the idea that modeling efforts must consider the source of aerosols deposited in different ocean regions, as well as the potential for future changes in the composition of aerosols entering the ocean.

3.4. Effect of Organic Ligands on Aerosol Iron Dissolution

Figure 5a shows the mean total dFe leached from aerosol sample AER 1 into ambient seawater and into seawater samples amended with various organic ligands. Despite the added ligands having very different conditional stability constants with respect to Fe complexation, the mean total dFe leached from aerosols

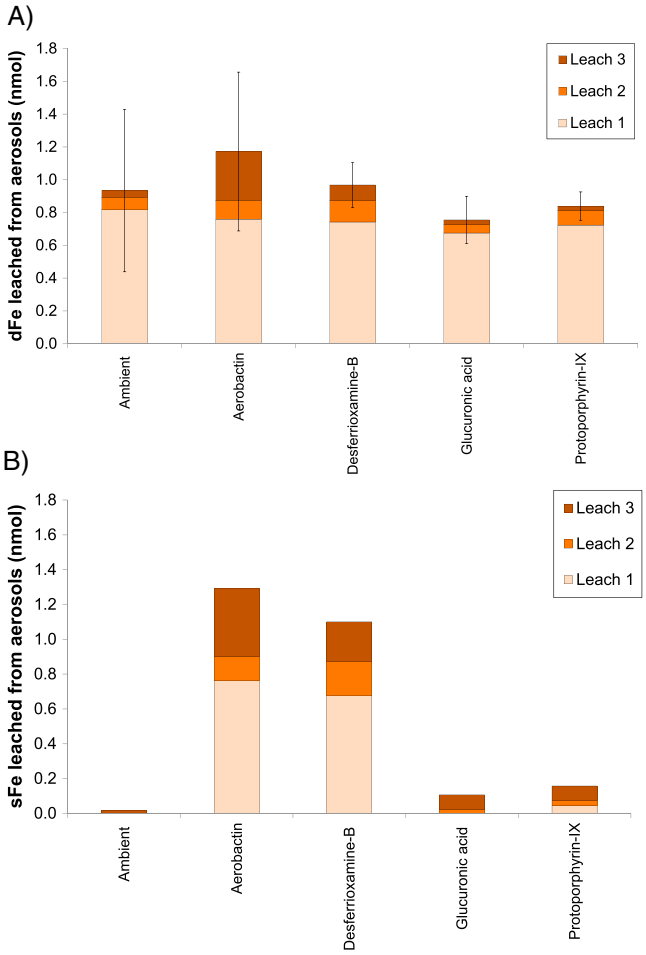

Figure 5. The mean total amount (nmol) of (a) dissolved iron (dFe) and (b) soluble iron (sFe) leached from aerosol sample AER 1 into ambient seawater and seawater amended with various Fe-binding organic ligands (aerobactin, desferrioxamine B, glucuronic acid, and protoporphyrin IX). Error bars in Figure 5a represent the standard deviation ($\pm 1\sigma$) on the mean total dFe leached from replicate subsamples of the same aerosol sample. No error bars are shown in Figure 5b, as replicate leaches were not performed. In both Figures 5a and 5b, the segments of each bar show the amount of dFe leached during each sequential aerosol leach (i.e., leaches 1–3). Sequential leaches 1, 2, and 3 represent the following time periods for seawater that was exposed to aerosols: 0–5 min, 5–10 min, and 10 min–48 h, respectively. Leach 4 was not performed in this experiment.

following all leaches (including a control using seawater with no added ligands) fell in the narrow range of 0.8 ± 0.1 nmol to 1.2 ± 0.5 nmol. Interestingly, there was no statistical difference between the mean total dFe leached into each ligand-amended seawater sample and that leached into unamended ambient seawater (two-tailed *t* test, $p > 0.05$), which contrasts with the results of previous work by *Aguilar-Islas et al.* [2010]. However, this earlier study did not include replicate leaches using subsamples of a single-aerosol sample. Our study has shown that the RSD associated with replicate leaches can exceed 50%, and while the mean total amounts of dFe leached into ligand-amended seawater appeared to differ from that leached into ambient seawater, these differences were not statistically significant. The majority of the variation in dFe leached from subsamples of a single-aerosol filter reflects either the inherent variability of the leaching process (i.e., the leaching mechanism or variability in the Fe species or particle character) or the heterogeneity of Fe species with different fractional solubilities across the aerosol filter. Bulk analysis of an extended suite of aerosol digest solutions (data not shown) suggests that heterogeneity in the total Fe contained on the aerosol filter is unlikely to be responsible for the observed variability in dFe between replicate leaches (RSD on the mean total Fe in subsamples of a single aerosol sample is $<3\%$).

In stark contrast, there were pronounced differences in the mean total sFe in leachate solutions after leaching with unamended ambient seawater versus seawater amended with the L_1-type ligands aerobactin and desferrioxamine B (Figure 5b). The mean total sFe leached into ambient seawater leachate was 0.02 nmol, whereas leachate from seawater amended with aerobactin and desferrioxamine B contained 1.3 nmol and 1.1 nmol sFe, respectively. This large impact observed with L_1-type ligand-amended seawater was not seen with the weaker organic ligands, glucuronic acid and protoporphyrin IX, for which leachate solutions contained 0.10 nmol and 0.16 nmol sFe, respectively.

In comparing the dFe and sFe in the seawater leachate solutions, it is apparent that the majority (~100%) of the dFe in ambient seawater leachate existed as cFe. The same was true for all of the seawater leachate solutions from the temperature, pH, and dissolved O_2 experiments. This observation is consistent with the results of previous laboratory studies and field observations [*Wu et al.*, 2001; *Bergquist et al.*, 2007; *Aguilar-Islas et al.*, 2010; *Ussher et al.*, 2013; *Fitzsimmons and Boyle*, 2014]. Conversely, for aerosols leached with seawater

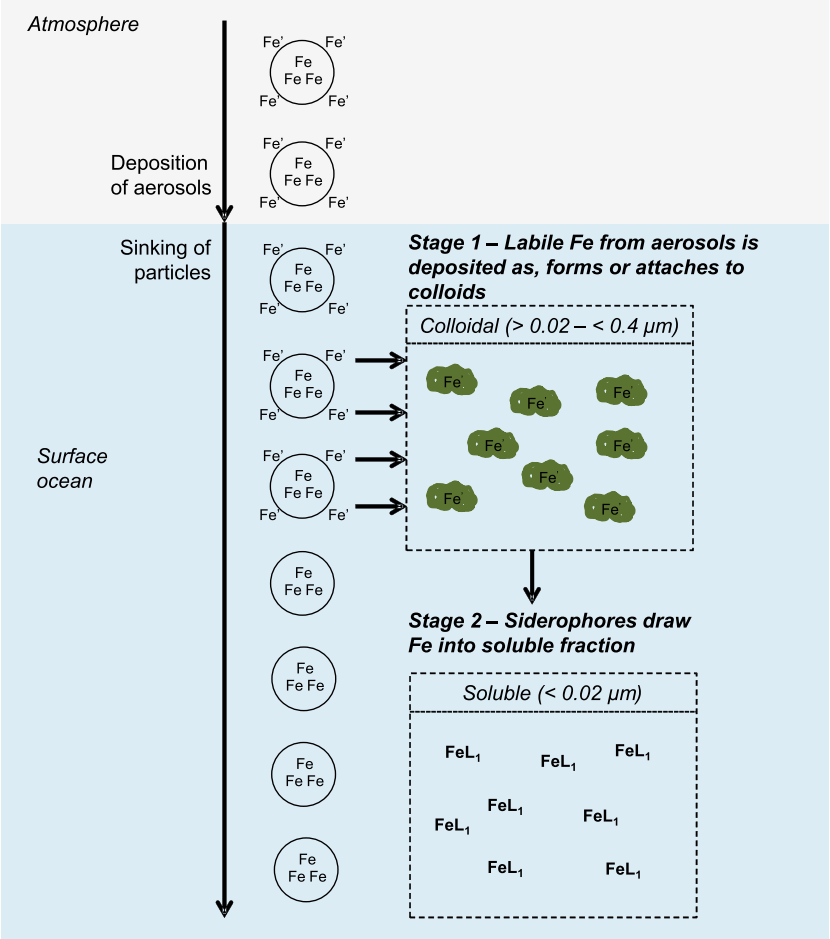

Figure 6. A conceptual model for the dissolution of aerosol iron (Fe) in surface ocean waters, which proposes a two-stage mechanism. Fe = refractory Fe species, Fe′ = labile Fe species, and FeL_1 = L_1Fe-ligand complexes.

amended with the L_1-type ligands aerobactin and desferrioxamine B, the majority of dFe in the leachate (77–98%) resided in the sFe fraction. However, for leaches with seawater amended with the weaker ligands, glucuronic acid and protoporphyrin IX, there was only a small increase in the proportion of sFe in the leachate compared with the control experiment using ambient conditions (sFe accounted for 11–21% of dFe). This observation suggests that the stronger L_1-type ligands may play an important role in the dissolution of aerosol Fe in the surface ocean.

Based on the results of this study, we hypothesize a two-stage mechanism for the dissolution of aerosol Fe in seawater (Figure 6). First, upon deposition of aerosols at the ocean surface, labile inorganic Fe [Fe(II) and Fe(III)] is released into seawater, whereupon it rapidly forms colloidal-sized ferric oxyhydroxides or is adsorbed or complexed by colloidal-sized organic matter with metal-binding functional groups (e.g., saccharides [*Hassler et al.*, 2011], amino acids [*Benner*, 2011], and humic substances [*Laglera and van den Berg*, 2009]). After this first stage, the dissolved aerosol Fe exists predominantly in the cFe size fraction, as observed in the majority of our experimental leachate solutions. During the second stage of our hypothesized mechanism, strong L_1-type ligands, such as siderophores, if present uncomplexed in sufficient concentration, form strong Fe-ligand complexes, whereby there is a transfer of dissolved aerosol Fe from the colloidal to the soluble size fraction, as low molecular weight (~300–1000 amu) Fe-ligand complexes [*Macrellis et al.*, 2001]. The fact that not all Fe is "solubilized" by L_1-type ligands, despite seawater being amended with large excess concentrations (10 n*M*) in our experiments, may reflect the physical or chemical association of some L_1-type ligands with colloidal material present in the seawater.

An alternative hypothesis is that upon deposition at the surface ocean, aerosols may release colloidal-sized organic matter or inorganic phases with which Fe is already associated [*Raiswell and Canfield*, 2012; *Paris and*

Desboeufs, 2013]. In seawater, L_1-type ligands can then draw the aeolian cFe into the soluble fraction, as described above. However, we suggest that it is more likely that dFe released from aerosols associates with colloids already present in seawater. This conclusion is based on results for the leaching of aerosols using seawater preconditioned by filtration (<0.4 μm) and ultrafiltration (<0.02 μm), which show lower dFe concentrations in leachate derived using ultrafiltered seawater [*Ussher*, 2005]. In addition, *Dammshäuser and Croot* [2012] showed that aerosol Al and titanium (Ti) colloidal associations are very low following dissolution into seawater compared to soluble forms, potentially indicating low input of colloidal matter from aerosols.

More work is required to establish whether colloidal Fe is delivered by aerosols or forms in seawater following deposition and determine if aerosol characteristics such as particle size of deposited aerosols and aerosol composition (i.e., mineral dust versus combustion products) play a role in this dissolution mechanism. Certainly, a higher proportion of colloidal Fe has been observed in regions of fine-mode aerosol deposition in comparison to regions of coarse-mode aerosol deposition, and this fine aerosol size fraction results in higher fractional solubilities of Fe [*Buck et al.*, 2010b; *Ussher et al.*, 2013].

In summary, from our experimental results, it seems clear that stronger organic Fe-binding ligands play an important role in the dissolution of aerosol Fe. This observation has important implications for our understanding of the biogeochemical role of organic ligands with regard to the cycling of Fe. In the absence of such organic ligands, aerosol-derived dFe will remain largely in the colloidal size fraction in seawater; in which case, it is expected to be more rapidly lost from surface ocean waters over a period of weeks to months [*Moran and Buesseler*, 1992; *Boyd et al.*, 2010]. In the presence of sufficient concentrations of strong ligands, however, aerosol-derived dFe may be transferred from the colloidal to the soluble size fraction, where it may be expected to have a longer residence time in the euphotic zone [*Boyd and Ellwood*, 2010] and thus have greater biological availability to phytoplankton. It is important to note that the role that biological organisms play in aerosol Fe dissolution has not been considered in this study and should be included when attempting to understand the complete aerosol Fe dissolution mechanism.

4. Conclusions

The results of this experimental study suggest that plausible future variations in the temperature, pH, and O_2 concentration of seawater will have a minor impact on the dissolution of aerosol Fe. However, in accord with other studies, our data indicate that aerosol composition has the most significant effect on the dissolution of aerosol Fe, with North Atlantic aerosol samples with the greatest anthropogenic components having the highest fractional solubility. Hence, we surmise that future increases in the magnitude of global aerosol fluxes and the proportion of combustion aerosols, relative to mineral dust, are likely to be the most important drivers of changes in the atmospheric flux of dFe to the surface ocean. Therefore, it is reasonable for modelers not to prioritize the inclusion of seawater temperature, pH, and O_2 concentration effects on aerosol Fe dissolution, but instead, focus attention on the regional differences in the original source of deposited aerosols.

Furthermore, our results highlight the importance of strong Fe-binding organic ligands in regulating the size distribution of aerosol-derived dFe in surface ocean waters, specifically in increasing the residence time and biological availability of aerosol-derived Fe in the surface ocean. A conceptual model of aerosol Fe dissolution is proposed in which strong Fe-binding organic ligands play a key role. The proposed two-stage mechanism highlights the significance of (i) the colloidal phase and (ii) the strong L_1-type ligands in the soluble phase in retaining biologically available aerosol Fe in surface ocean waters following aerosol deposition.

Acknowledgments
This research was supported by a European Commission Marie Curie International Outgoing Fellowship for S.J.U. (PIOF-GA-2009-235418 SOLAIROS), a European Commission Marie Curie Career Integration Grant for S.J.U. (PCIG-GA-2012-333143 DISCOSAT), a Natural Environment Research Council (NERC) PhD studentship for M.P.F. (NE/J500380/1), a NERC grant for M.C.L. (NE/G016267/1), a National Science Foundation (NSF) grant for P.N.S. (OCE 0222053), a NSF grant for K.N.B. (OCE 0927453), and a NSF grant for T.M.C. (OCE 0222046). The authors would like to acknowledge Andrew Peters, Nicholas Bates, and Samantha de Putron (the Bermuda Institute of Ocean Science, BIOS) for all their support in this project and thank BIOS for a grant-in-aid. The authors also thank three anonymous reviewers for their constructive comments on the manuscript. Data to support this article are available directly from the corresponding author, Simon Ussher (sussher@plymouth.ac.uk).

References

Aguilar-Islas, A. M., J. Wu, R. Rember, A. M. Johansen, and L. M. Shank (2010), Dissolution of aerosol-derived iron in seawater: Leach solution chemistry, aerosol type, and colloidal iron fraction, *Mar. Chem.*, *120*(1–4), 25–33, doi:10.1016/j.marchem.2009.01.011.

Anderson, J. R., P. R. Buseck, T. L. Patterson, and R. Arimoto (1996), Characterization of the Bermuda tropospheric aerosol by combined individual-particle and bulk-aerosol analysis, *Atmos. Environ.*, *30*(2), 319–338, doi:10.1016/1352-2310(95)00170-4.

Aumont, O., E. Maier-Reimer, S. Blain, and P. Monfray (2003), An ecosystem model of the global ocean including Fe, Si, P colimitations, *Global Biogeochem. Cycles*, *17*(2), 1060, doi:10.1029/2001GB001745.

Baker, A. R., and P. L. Croot (2010), Atmospheric and marine controls on aerosol iron solubility in seawater, *Mar. Chem.*, *120*(1–4), 4–13, doi:10.1016/j.marchem.2008.09.003.

Baker, A. R., and T. D. Jickells (2006), Mineral particle size as a control on aerosol iron solubility, *Geophys. Res. Lett.*, *33*, L17608. doi:10.1029/2006GL026557.

Baker, A. R., T. D. Jickells, K. F. Biswas, K. Weston, and M. French (2006), Nutrients in atmospheric aerosol particles along the Atlantic Meridional Transect, *Deep Sea Res. Topic. Stud. Oceanogr.*, *53*(14–16), 1706–1719, doi:10.1016/j.dsr2.2006.05.012.

Baker, A. R., C. Adams, T. G. Bell, T. D. Jickells, and L. Ganzeveld (2013), Estimation of atmospheric nutrient inputs to the Atlantic Ocean from 50°N to 50°S based on large-scale field sampling: Iron and other dust-associated elements, *Global Biogeochem. Cycles*, *27*, 755–767, doi:10.1002/gbc.20062.

Benner, R. (2011), Loose ligands and available iron in the ocean, *Proc. Natl. Acad. Sci.*, *108*(3), 893–894, doi:10.1073/pnas.1018163108.

Bergquist, B. A., J. Wu, and E. A. Boyle (2007), Variability in oceanic dissolved iron is dominated by the colloidal fraction, *Geochim. Cosmochim. Acta*, *71*(12), 2960–2974, doi:10.1016/j.gca.2007.03.013.

Bonnet, S., and C. Guieu (2004), Dissolution of atmospheric iron in seawater, *Geophys. Res. Lett.*, *31*, L03303, doi:10.1029/2003GL018423.

Boyd, P. W., and M. J. Ellwood (2010), The biogeochemical cycle of iron in the ocean, *Nat. Geosci.*, *3*(10), 675–682, doi:10.1038/ngeo964.

Boyd, P. W., et al. (2000), A mesoscale phytoplankton bloom in the polar Southern Ocean stimulated by iron fertilization, *Nature*, *407*(6805), 695–702, doi:10.1038/35037500.

Boyd, P. W., E. Ibisanmi, S. G. Sander, K. A. Hunter, and G. A. Jackson (2010), Remineralization of upper ocean particles: Implications for iron biogeochemistry, *Limnol. Oceanogr.*, *55*(3), 1271–1288, doi:10.4319/lo.2010.55.3.1271.

Breitbarth, E., R. Bellerby, C. Neill, M. Ardelan, M. Meyerhöfer, E. Zöllner, P. Croot, and U. Riebesell (2010), Ocean acidification affects iron speciation during a coastal seawater mesocosm experiment, *Biogeosciences*, *7*(3), 1065–1073, doi:10.5194/bg-7-1065-2010.

Buck, C. S., W. M. Landing, J. A. Resing, and G. T. Lebon (2006), Aerosol iron and aluminum solubility in the northwest Pacific Ocean: Results from the 2002 IOC cruise, *Geochem. Geophys. Geosyst.*, *7*, Q04M07, doi:10.1029/2005GC000977.

Buck, C. S., W. M. Landing, and J. A. Resing (2010a), Particle size and aerosol iron solubility: A high-resolution analysis of Atlantic aerosols, *Mar. Chem.*, *120*(1–4), 14–24, doi:10.1016/j.marchem.2008.11.002.

Buck, C. S., W. M. Landing, J. A. Resing, and C. I. Measures (2010b), The solubility and deposition of aerosol Fe and other trace elements in the North Atlantic Ocean: Observations from the A16N CLIVAR/CO2 repeat hydrography section, *Mar. Chem.*, *120*(1–4), 57–70, doi:10.1016/j.marchem.2008.08.003.

Buck, C. S., W. M. Landing, and J. Resing (2013), Pacific Ocean aerosols: Deposition and solubility of iron, aluminum, and other trace elements, *Mar. Chem.*, *157*, 117–130, doi:10.1016/j.marchem.2013.09.005.

Buck, K. N., B. Sohst, and P. N. Sedwick (2014), The organic complexation of dissolved iron along the U.S. GEOTRACES North Atlantic Section, *Deep Sea Res. II*, in press.

Byrne, R. H., and D. R. Kester (1976), Solubility of hydrous ferric oxide and iron speciation in seawater, *Mar. Chem.*, *4*(3), 255–274, doi:10.1016/0304-4203(76)90012-8.

Caldeira, K., and M. E. Wickett (2003), Oceanography: Anthropogenic carbon and ocean pH, *Nature*, *425*(6956), 365, doi:10.1038/425365a.

Chen, L., and R. A. Duce (1983), The sources of sulfate, vanadium and mineral matter in aerosol particles over Bermuda, *Atmos. Environ.*, *17*(10), 2055–2064, doi:10.1016/0004-6981(83)90362-1.

Chen, Y., and R. L. Siefert (2004), Seasonal and spatial distributions and dry deposition fluxes of atmospheric total and labile iron over the tropical and subtropical North Atlantic Ocean, *J. Geophys. Res.*, *109*, D09305, 10.1029/2003JD003958.

Coale, K. H., et al. (1996), A massive phytoplankton bloom induced by an ecosystem-scale iron fertilization experiment in the equatorial Pacific Ocean, *Nature*, *383*(6600), 495–501, doi:10.1038/383495a0.

Croot, P. L., A. R. Bowie, R. D. Frew, M. T. Maldonado, J. A. Hall, K. A. Safi, J. La Roche, P. W. Boyd, and C. S. Law (2001), Retention of dissolved iron and Fe II in an iron induced Southern Ocean phytoplankton bloom, *Geophys. Res. Lett.*, *28*(18), 3425–3428, doi:10.1029/2001GL013023.

Cullen, J. T., B. A. Bergquist, and J. W. Moffett (2006), Thermodynamic characterization of the partitioning of iron between soluble and colloidal species in the Atlantic Ocean, *Mar. Chem.*, *98*(2–4), 295–303, doi:10.1016/j.marchem.2005.10.007.

Cutter, G., P. Andersson, L. Codispoti, P. Croot, R. Francois, M. Lohan, H. Obata, and M. Rutgers vd Loeff (2010), Sampling and sample-handling protocols for GEOTRACES Cruises *Rep*., GEOTRACES, Toulouse, France.

Dammshäuser, A., and P. L. Croot (2012), Low colloidal associations of aluminium and titanium in surface waters of the tropical Atlantic, *Geochim. Cosmochim. Acta*, *96*(0), 304–318, doi:10.1016/j.gca.2012.07.032.

de Putron, S. J., D. C. McCorkle, A. L. Cohen, and A. Dillon (2011), The impact of seawater saturation state and bicarbonate ion concentration on calcification by new recruits of two Atlantic corals, *Coral Reefs*, *30*, 321–328, doi:10.1007/s00338-010-0697-z.

Desboeufs, K. V., A. Sofikitis, R. Losno, J. L. Colin, and P. Ausset (2005), Dissolution and solubility of trace metals from natural and anthropogenic aerosol particulate matter, *Chemosphere*, *58*(2), 195–203, doi:10.1016/j.chemosphere.2004.02.025.

Duce, R. A. (1986), The impact of atmospheric nitrogen, phosphorus, and iron species on marine biological productivity, in *The Role of Air-Sea Exchange in Geochemical Cycling*, edited by P. Buat-Ménard, pp. 497–529, Springer, Netherlands.

Duce, R. A., and G. L. Hoffman (1976), Atmospheric vanadium transport to the ocean, *Atmos. Environ.*, *10*(11), 989–996, doi:10.1016/0004-6981(76)90207-9.

Fitzsimmons, J. N., and E. A. Boyle (2014), Both soluble and colloidal iron phases control dissolved iron variability in the tropical North Atlantic Ocean, *Geochim. Cosmochim. Acta*, *125*(0), 539–550, doi: 10.1016/j.gca.2013.10.032.

Gledhill, M., and K. N. Buck (2012), The organic complexation of iron in the marine environment: A review, *Front. Microbiol.*, *3*, doi:10.3389/fmicb.2012.00069.

Hassler, C. S., V. Schoemann, C. M. Nichols, E. C. Butler, and P. W. Boyd (2011), Saccharides enhance iron bioavailability to Southern Ocean phytoplankton, *Proc. Natl. Acad. Sci.*, *108*(3), 1076–1081, doi:10.1073/pnas.1010963108.

Hopkinson, B. M., and K. A. Barbeau (2007), Organic and redox speciation of iron in the eastern tropical North Pacific suboxic zone, *Mar. Chem.*, *106*(1–2), 2–17, doi:10.1016/j.marchem.2006.02.008.

Hsu, S.-C., et al. (2010), Sources, solubility, and dry deposition of aerosol trace elements over the East China Sea, *Mar. Chem.*, *120*(1–4), 116–127, doi:10.1016/j.marchem.2008.10.003.

Hunter, K. A., and P. W. Boyd (2007), Iron-binding ligands and their role in the ocean biogeochemistry of iron, *Environ. Chem.*, *4*(4), 221–232, doi:10.1071/EN07012.

International Energy Agency (2009), World Energy Outlook 2009 *Rep*, International Energy Agency, Cedex.

Intergovernmental Panel on Climate Change (2013), Working Group I Contribution to the IPCC Fifth Assessment Report Climate Change 2013: The Physical Science Basis, Summary for Policymakers *Rep*, IPCC, Geneva, Switzerland.

Jang, H.-N., Y.-C. Seo, J.-H. Lee, K.-W. Hwang, J.-I. Yoo, C.-H. Sok, and S.-H. Kim (2007), Formation of fine particles enriched by V and Ni from heavy oil combustion: Anthropogenic sources and drop-tube furnace experiments, *Atmos. Environ.*, *41*(5), 1053–1063, doi:10.1016/j.atmosenv.2006.09.011.

Jickells, T. D., et al. (2005), Global iron connections between desert dust, ocean biogeochemistry, and climate, *Science*, *308*(5718), 67–71, doi:10.1126/science.1105959.

Kohfeld, K. E., and A. Ridgwell (2009), Glacial-interglacial variability in atmospheric CO_2, *Geophys. Monogr. Ser.*, *187*, 251–286, doi:10.1029/2008GM000845.
Kuma, K., J. Nishioka, and K. Matsunaga (1996), Controls on iron (III) hydroxide solubility in seawater: The influence of pH and natural organic chelators, *Limnol. Oceanogr.*, *41*(3), 396–407, doi:10.4319/lo.1996.41.3.0396.
Laglera, L. M., and C. M. G. van den Berg (2009), Evidence for geochemical control of iron by humic substances in seawater, *Limnol. Oceanogr.*, *54*(2), 610–619, doi:10.4319/lo.2009.54.2.0610.
Liu, X., and F. J. Millero (1999), The solubility of iron hydroxide in sodium chloride solutions, *Geochim. Cosmochim. Acta*, *63*(19–20), 3487–3497, doi:10.1016/S0016-7037(99)00270-7.
Liu, X., and F. J. Millero (2002), The solubility of iron in seawater, *Mar. Chem.*, *77*(1), 43–54, doi:10.1016/S0304-4203(01)00074-3.
Macrellis, H. M., C. G. Trick, E. L. Rue, G. Smith, and K. W. Bruland (2001), Collection and detection of natural iron-binding ligands from seawater, *Mar. Chem.*, *76*(3), 175–187, doi:10.1016/S0304-4203(01)00061-5.
Martin, J. H. (1990), Glacial-Interglacial CO_2 Change: The Iron Hypothesis, *Paleoceanography*, *5*(1), 1–13, doi:10.1029/PA005i001p00001.
Martin, J. H., and M. R. Gordon (1988), Northeast Pacific iron distributions in relation to phytoplankton productivity, *Deep Sea Res. Oceanogr. Res. Pap.*, *35*(2), 177–196, doi:10.1016/0198-0149(88)90035-0.
Martin, J. H., et al. (1994), Testing the iron hypothesis in ecosystems of the equatorial Pacific Ocean, *Nature*, *371*(6493), 123–129, doi:10.1038/371123a0.
Meehl, G. A., et al. (Eds.) (2007), *Global Climate Projections*, Cambridge Univ. Press, Cambridge, U. K.
Meskhidze, N., A. Nenes, W. C. Conant, and J. H. Seinfeld (2005), Evaluation of a new cloud droplet activation parameterization with in situ data from CRYSTAL-FACE and CSTRIPE, *J. Geophys. Res.*, *110*, D16202. doi:10.1029/2004JD005703.
Millero, F. J., S. Sotolongo, and M. Izaguirre (1987), The oxidation kinetics of Fe(II) in seawater, *Geochim. Cosmochim. Acta*, *51*(4), 793–801, doi:10.1016/0016-7037(87)90093-7.
Millero, F. J., R. Woosley, B. DiTrolio, and J. Waters (2009), Effect of ocean acidification on the speciation of metals in seawater, *Oceanography*, *22*, 72–85, doi:10.5670/oceanog.2009.98.
Moore, J. K., S. C. Doney, and K. Lindsay (2004), Upper ocean ecosystem dynamics and iron cycling in a global three-dimensional model, *Global Biogeochem. Cycles*, *18*, GB4028. doi:10.1029/2004GB002220.
Moran, S. B., and K. O. Buesseler (1992), Short residence time of colloids in the upper ocean estimated from ^{238}U-^{234}Th disequilibria, *Nature*, *359*(6392), 221–223, doi:10.1038/359221a0.
Morton, P. L., W. M. Landing, S.-C. Hsu, A. Milne, A. M. Aguilar-Islas, A. R. Baker, A. R. Bowie, C. S. Buck, Y. Gao, and S. Gichuki (2013), Methods for the sampling and analysis of marine aerosols: Results from the 2008 GEOTRACES aerosol intercalibration experiment, *Limnolol. Oceanogr. Meth.*, *11*, 62–78, doi:10.4319/lom.2013.11.62.
Oakes, M., R. Weber, B. Lai, A. Russell, and E. Ingall (2012), Characterization of iron speciation in urban and rural single particles using XANES spectroscopy and micro X-ray fluorescence measurements: Investigating the relationship between speciation and fractional iron solubility, *Atmos. Chem. Phys.*, *12*(2), 745–756, doi:10.5194/acp-12-745-2012.
Obata, H., H. Karatani, and E. Nakayama (1993), Automated determination of iron in seawater by chelating resin concentration and chemiluminescence detection, *Anal. Chem.*, *65*(11), 1524–1528, doi:10.1021/ac00059a007.
Orr, J. C., V. J. Fabry, O. Aumont, L. Bopp, S. C. Doney, R. A. Feely, A. Gnanadesikan, N. Gruber, A. Ishida, and F. Joos (2005), Anthropogenic ocean acidification over the twenty-first century and its impact on calcifying organisms, *Nature*, *437*(7059), 681–686, doi:10.1038/nature04095.
Parekh, P., M. J. Follows, and E. A. Boyle (2005), Decoupling of iron and phosphate in the global ocean, *Global Biogeochem. Cycles*, *19*, GB2020, doi:10.1029/2004GB002280.
Paris, R., and K. V. Desboeufs (2013), Effect of atmospheric organic complexation on iron-bearing dust solubility, *Atmos. Chem. Phys.*, *13*(9), 4895–4905, doi:10.5194/acp-13-4895-2013.
Prospero, J. M., P. Ginoux, O. Torres, S. E. Nicholson, and T. E. Gill (2002), Environmental characterization of global sources of atmospheric soil dust identified with the Nimbus 7 Total Ozone Mapping Spectrometer (TOMS) absorbing aerosol product, *Rev. Geophys.*, *40*(1), 1002, doi:10.1029/2000RG000095.
Raiswell, R., and D. E. Canfield (2012), The iron biogeochemical cycle past and present, *Geochem. Perspect.*, *1*(1), 1–322, doi:10.7185/geochempersp.1.1.
Rose, A. L., and T. D. Waite (2001), Chemiluminescence of luminol in the presence of iron(II) and oxygen: Oxidation mechanism and implications for its analytical use, *Anal. Chem.*, *73*(24), 5909–5920, doi:10.1021/ac015547q.
Rue, E. L., and K. W. Bruland (1995), Complexation of iron(III) by natural organic ligands in the Central North Pacific as determined by a new competitive ligand equilibration/adsorptive cathodic stripping voltammetric method, *Mar. Chem.*, *50*(1–4), 117–138, doi:10.1016/0304-4203(95)00031-l.
Sedwick, P. N., T. M. Church, A. R. Bowie, C. M. Marsay, S. J. Ussher, K. M. Achilles, P. J. Lethaby, R. J. Johnson, M. M. Sarin, and D. J. McGillicuddy (2005), Iron in the Sargasso Sea (Bermuda Atlantic Time-series Study region) during summer: Eolian imprint, spatiotemporal variability, and ecological implications, *Global Biogeochem. Cycles*, *19*, GB4006, doi:10.1029/2004GB002445.
Sedwick, P. N., E. R. Sholkovitz, and T. M. Church (2007), Impact of anthropogenic combustion emissions on the fractional solubility of aerosol iron: Evidence from the Sargasso Sea, *Geochem. Geophys. Geosyst.*, *8*, Q10Q06, doi:10.1029/2007GC001586.
Séguret, M. J. M., M. Koçak, C. Theodosi, S. J. Ussher, P. J. Worsfold, B. Herut, N. Mihalopoulos, N. Kubilay, and M. Nimmo (2011), Iron solubility in crustal and anthropogenic aerosols: The Eastern Mediterranean as a case study, *Mar. Chem.*, *126*(1–4), 229–238, doi:10.1016/j.marchem.2011.05.007.
Shaffer, G., S. M. Olsen, and J. O. P. Pedersen (2009), Long-term ocean oxygen depletion in response to carbon dioxide emissions from fossil fuels, *Nat. Geosci.*, *2*(2), 105–109, doi:10.1038/ngeo420.
Shelley, R., P. N. Sedwick, T. Bibby, P. Cabedo-Sanz, T. M. Church, R. J. Johnson, A. Macey, C. Marsay, E. R. Sholkovitz, and S. J. Ussher (2012), Controls on dissolved cobalt in surface waters of the Sargasso Sea: Comparisons with iron and aluminum, *Global Biogeochem. Cycles*, *26*, GB2020, doi:10.1029/2011GB004155.
Sholkovitz, E. R., P. N. Sedwick, and T. M. Church (2009), Influence of anthropogenic combustion emissions on the deposition of soluble aerosol iron to the ocean: Empirical estimates for island sites in the North Atlantic, *Geochim. Cosmochim. Acta*, *73*(14), 3981–4003, doi:10.1016/j.gca.2009.04.029.
Sholkovitz, E. R., P. N. Sedwick, T. M. Church, A. R. Baker, and C. F. Powell (2012), Fractional solubility of aerosol iron: Synthesis of a global-scale data set, *Geochim. Cosmochim. Acta*, *89*, 173–189, doi:10.1016/j.gca.2012.04.022.
Stramma, L., G. C. Johnson, J. Sprintall, and V. Mohrholz (2008), Expanding oxygen-minimum zones in the tropical oceans, *Science*, *320*(5876), 655–658, doi:10.1126/science.1153847.
Tagliabue, A., L. Bopp, O. Aumont, and K. R. Arrigo (2009), Influence of light and temperature on the marine iron cycle: From theoretical to global modeling, *Global Biogeochem. Cycles*, *23*, GB2017, doi:10.1029/2008GB003214.

Takeda, S., and A. Tsuda (2005), An in situ iron-enrichment experiment in the western subarctic Pacific (SEEDS): Introduction and summary, *Prog. Oceanogr.*, *64*(2–4), 95–109, doi:10.1016/j.pocean.2005.02.004.

Taylor, S. R., and S. M. McLennan (1995), The geochemical evolution of the continental crust, *Rev. Geophys.*, *33*(2), 241–265, doi:10.1029/95RG00262.

Ussher, S. (2005), Determination of dissolved iron speciation in the North East Atlantic Ocean by flow injection chemiluminescence, PhD thesis, School of Geography, Earth and Environmental Sciences, Plymouth Univ., Plymouth, U. K.

Ussher, S. J., E. P. Achterberg, G. Sarthou, P. Laan, H. J. W. de Baar, and P. J. Worsfold (2010), Distribution of size fractionated dissolved iron in the Canary Basin, *Mar. Environ. Res.*, *70*(1), 46–55, doi:10.1016/j.marenvres.2010.03.001.

Ussher, S. J., E. P. Achterberg, C. Powell, A. R. Baker, T. D. Jickells, R. Torres, and P. J. Worsfold (2013), Impact of atmospheric deposition on the contrasting iron biogeochemistry of the North and South Atlantic Ocean, *Global Biogeochem. Cycles*, *27*, 1096–1107, doi:10.1002/gbc.20056.

Whitney, F. A., H. J. Freeland, and M. Robert (2007), Persistently declining oxygen levels in the interior waters of the eastern subarctic Pacific, *Prog. Oceanogr.*, *75*(2), 179–199, doi:10.1016/j.pocean.2007.08.007.

Wozniak, A. S., R. U. Shelley, R. L. Sleighter, H. A. N. Abdulla, P. L. Morton, W. M. Landing, and P. G. Hatcher (2013), Relationships among aerosol water soluble organic matter, iron and aluminum in European, North African, and Marine air masses from the 2010 US GEOTRACES cruise, *Mar. Chem.*, *154*, 24–33, doi:10.1016/j.marchem.2013.04.011.

Wu, J., E. Boyle, W. Sunda, and L.-S. Wen (2001), Soluble and colloidal iron in the oligotrophic North Atlantic and North Pacific, *Science*, *293*(5531), 847–849, doi:10.1126/science.1059251.

Wu, J., R. Rember, and C. Cahill (2007), Dissolution of aerosol iron in the surface waters of the North Pacific and North Atlantic oceans as determined by a semicontinuous flow-through reactor method, *Global Biogeochem. Cycles*, *21*, GB4010, doi:10.1029/2006GB002851.

Zhu, X. R., J. M. Prospero, and F. J. Millero (1997), Diel variability of soluble Fe(II) and soluble total Fe in North African dust in the trade winds at Barbados, *J. Geophys. Res.*, *102*(D17), 21,297–21,305, doi:10.1029/97JD01313.

Zhuang, G., R. A. Duce, and D. R. Kester (1990), The dissolution of atmospheric iron in surface seawater of the open ocean, *J. Geophys. Res.*, *95*(C9), 16,207–16,216, doi:10.1029/JC095iC09p16207.